

ARTICLE

OPEN

Connecting the dots: NO_x emissions along a West Siberian natural gas pipeline

R. J. van der A  , A. T. J. de Laat¹, J. Ding  and H. J. Eskes¹

New high quality satellite measurements of nitrogen dioxide (NO_2) of the TROPOspheric Monitoring Instrument (TROPOMI) over snow-covered regions of Siberia reveal previously undocumented but significant NO_2 emissions associated with the natural gas industry in Western Siberia. Besides gas drilling and natural gas power plants, also gas compressor stations for the transport of natural gas are sources of high amounts of nitrogen oxides ($\text{NO}_x = \text{NO} + \text{NO}_2$), which are emitted in otherwise pristine regions. The emissions per station from these remote gas compressor stations are at least an order of magnitude larger than those reported for North American gas compressor stations, possibly related to less stringent environmental regulations in Siberia compared to the United States. This discovery was made possible thanks to a newly developed technique for discriminating snow covered surfaces from clouds, which allows for satellite measurements of tropospheric NO_2 columns over large boreal snow-covered areas. While retrievals over snow-covered areas were traditionally filtered out, we used the retrieved column of air in these observations to distinguish clouds higher in the atmosphere from the snow at the surface. This results in 23% more TROPOMI observations on an annual basis. Furthermore, these observations have a precision four times better than nearly any TROPOMI observation over other areas and surfaces around the world. These new results highlight the potential of TROPOMI on Sentinel 5P as well as future satellite missions for monitoring small-scale emissions and emissions at high latitudes.

npj Climate and Atmospheric Science (2020)3:16; <https://doi.org/10.1038/s41612-020-0119-z>

INTRODUCTION

Measuring atmospheric composition from space using satellites has been expanding rapidly over the last two decades with the launch of the first generation of environmental satellites like ENVISAT, AURA and a host of other satellites. Currently, instruments like TROPOspheric Monitoring Instrument (TROPOMI)¹ measure a wide variety of atmospheric trace gases on a daily basis, including gases relevant for monitoring air quality², like NO_2 , carbon monoxide (CO), and sulfur dioxide (SO_2). These satellite measurements have proven their value during the last two decades not only for monitoring atmospheric composition and air quality worldwide, but also for independently determining trace gas emissions, whose reporting is often mandatory as part of emission regulations^{3–5}. For example, satellite observations reveal that since the mid-2000s emissions of NO_2 in the United States and in Europe have been steadily decreasing, confirming that air quality policies and measures have been effective^{6–8}. On the other hand, emissions in South, Southeast, and East Asia have increased significantly due to increasing wealth, increasing populations, and increasing energy use^{9–14}. The recognition by the Chinese government of air quality as an important environmental hazard has also led to policies aimed at reducing SO_2 and NO_2 emissions^{7,15–17}. In the past 10 years, satellite observations have shown that emissions of both SO_2 and NO_2 have started to decrease¹⁷, most spectacularly for SO_2 , whose emissions in China have decreased by more than 70% between 2007 and 2016⁹.

In large part thanks to the success of the first generation environmental satellites, space agencies worldwide have started to plan for new environmental satellite missions. These missions incorporate the valuable lessons learned from the past 20 years while focusing on improving the satellites in order to better serve society. The current focus lies on improving spatial-temporal

resolution and signal-to-noise for the second generation of environmental satellite emissions. The European Space Agency Sentinel-5 Precursor (S5P) mission, with TROPOMI¹ onboard, launched October 2017, is one of the first such new satellites, providing high quality measurements of for example NO_2 at a high spatial resolution down to $3 \times 5.5 \text{ km}^2$. The satellite provides daily global coverage and higher frequencies towards the poles.

TROPOMI allows for more detailed and source specific monitoring of trace gas emissions¹⁸, as well as independent assessments of reported emissions. There is a particular interest in monitoring air quality and emissions of NO_2 , SO_2 , and CO, and greenhouse gas emissions like CO_2 and CH_4 , of localized sources from the oil and gas industry as well as the power generation industry, which often takes place at remote locations where possibilities for independent in situ monitoring can be limited. Furthermore, the prospect of accurately monitoring other emissions like NO_2 and CO allows for either indirectly determining CO_2 emissions using NO_2 or CO as proxies, or use NO_2 as a marker for emission from industrial complexes¹⁸.

The Urengoy natural gas field in West Siberia, discovered¹⁹ in 1966, is a prime example of oil and gas exploration at a remote and relatively inaccessible location. It is the second largest natural gas field in the world. Each year the gas field produces close to 500 billion cubic meters of gas of which about half is exported to Europe, which is about 40% of the total natural gas used in Europe. This transport takes place via the SRTO-Torzhok pipeline.

RESULTS

Cloud-snow differentiation

In this paper we study the effect of natural gas extraction and especially transport with the West Siberian pipeline on air quality.

¹Royal Netherlands Meteorological Institute (KNMI), De Bilt, The Netherlands. ²Nanjing University of Information Science & Technology (NUIST), Nanjing, China.  email: Ronald.van.der.A@knmi.nl

Due to its long distance transport, compression stations were built at regular spatial distances (~50–100 km) along the pipeline. These compressor stations burn natural gas for running turbines, leading to NO_x emissions.

Observations of the Ozone Monitoring Instrument (OMI) on the EOS-AURA satellite—launched in 2003 but still operational—and widely used for monitoring NO_2 from space⁷, are not sufficiently accurate to derive the NO_x emissions from relatively small sources like compression stations, because of the low signal-to-noise ratio in combination with a too coarse spatial resolution. NO_x emissions can be derived more accurately and with a higher spatial resolution using the NO_2 observations of TROPOMI.

However, regardless of the improvements of TROPOMI over OMI, large areas around the world at high latitudes—like Western Siberia—cannot be monitored during winter and spring due to the snow cover (see Fig. 1). Satellite instruments like OMI and TROPOMI use reflected visible solar radiation and are unable to distinguish between clouds and snow, which are equally bright for visible radiation (see methods). Hence, in current OMI and TROPOMI NO_2 retrieval algorithms, snow covered areas are flagged and filtered out. However, a new Cloud-Snow Differentiation method (CSD; see methods) allows to use satellites for measuring NO_2 over snow covered surfaces.

With the CSD method the number of useful pixels for TROPOMI increases globally with 6–39% per month depending on the season as shown in Table 1 and Fig. 1 (similar for OMI in Supplementary Fig. 1). Furthermore, not only does the number of pixels increase, these additional observations are of a better quality because of the very high reflectance of snow or ice (~0.8) resulting in a larger signal (~ factor 16) better than non-snow covered surfaces (reflectance ~0.05). Since the noise scales with the square-root of the signal, this typically leads to a factor four times better precision for these snow/ice measurements compared to measurements over non-snow surfaces.

TROPOMI measurements

Figure 2 shows a single day of TROPOMI observations over West Siberia, and reveals the major sources of NO_2 along the SRTO-Torzhok gas pipeline. The first six identified compressor stations

along the gas pipeline are indicated by numbers. Each location has been visually verified using GoogleEarth (Supplementary Fig. 2). Power plants in the region are indicated with the characters A to F. Most notable are the power plants GRES-1 (A) and GRES-2 (B) in Surgut, a city with a population of about 350,000. GRES-2 is the largest gas-fired power plant in the world⁶. Close to GRES-2 power plant is another smaller gas-fired power plant called CCGT, which in this study is combined with GRES-2 as they are located in the same emission inversion grid cell. GRES-1 is very close to GRES-2 but located in the adjacent grid cell. The only coal power plant is Vorkutinskaya (F) next to the town Vorkuta.

Figure 3 shows the monthly mean NO_2 concentrations observed by TROPOMI over the selected region throughout a year. For the months November to January there are almost no observations because of the polar night. The four months from February to May with snow cover clearly show the NO_2 enhancements from the compressor stations. During the snow-free summer period from June to September these NO_2 enhancements disappear due to the worse signal-to-noise ratio of the TROPOMI NO_2 measurements (reduced surface reflectance). Furthermore, NO_2 is more difficult to observe during summer months due to the shorter atmospheric lifetime of NO_2 and thus smaller concentrations. At the same time, biogenic NO_x emissions from the defrosted soil will increase during summer and further obscure small anthropogenic sources. By the end of September snow will invariably start covering the surface in this area and by October satellite measurement precision should have improved. However, from that moment the advance of the Polar night and rather high solar zenith angles start to limit the availability of TROPOMI measurements. The spring period is thus the best period for estimating emissions.

Emission estimates

Figure 4 shows the derived average NO_x emissions for April 2019 derived with the DECSO (Daily Emission estimation Constrained by Satellite Observations²⁰) algorithm (see methods section) as well as corresponding NO_x emissions from the Hemispheric Transport of Air Pollution bottom-up emission inventory (HTAP²¹). Apart from the sources identified in Fig. 2, strong emissions are detected in the North East corner of the map, where many drilling and

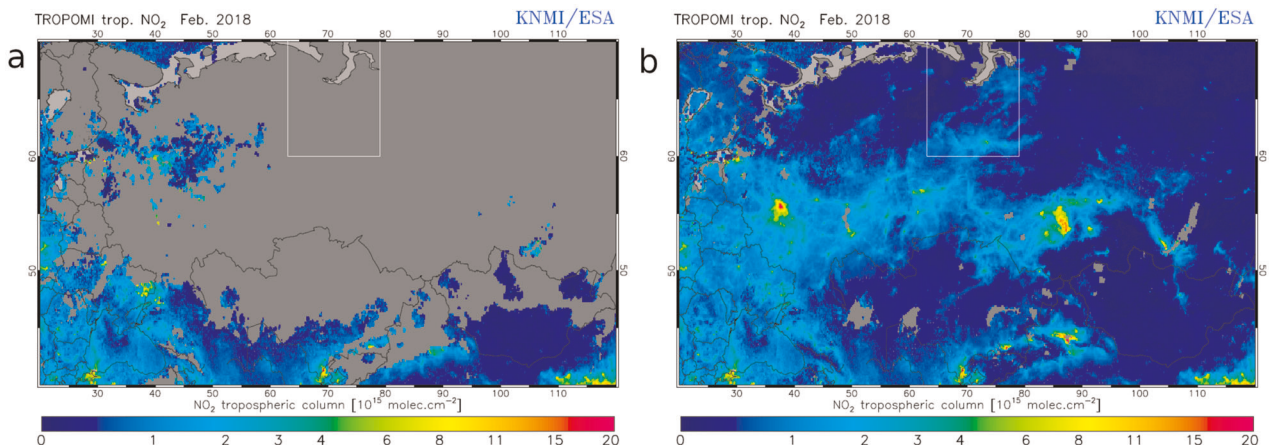


Fig. 1 Monthly mean NO_2 observations of TROPOMI for February 2018. a Without CSD method applied. **b** With the CSD method applied. The area of our research is indicated by the white box.

Table 1. The number of additional observations by applying the CSD method.

Jan.	Feb.	Mar.	Apr.	May	June	July	Aug.	Sep.	Oct.	Nov.	Dec.
36%	27%	25%	29%	28%	17%	8%	6%	6%	17%	33%	39%

14 Apr 2019

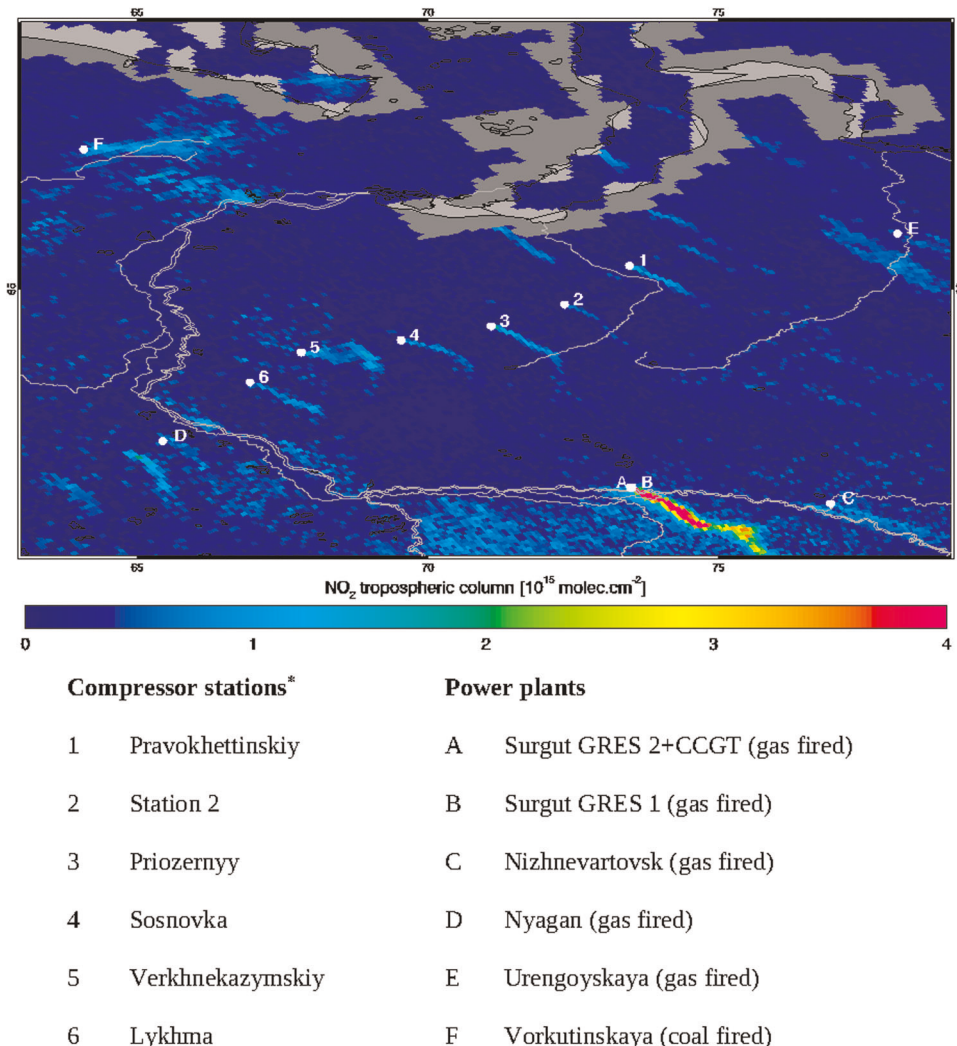


Fig. 2 NO₂ concentrations over West Siberia observed by TROPOMI on 14 April 2019. The main point sources in the region are indicated by numbers (for the compressor stations) and characters (for power plants). The inset shows the SRTO-Torzhok natural gas pipeline (orange) transport natural gas from the region around Urengoy in West Siberia to the various European natural gas pipelines. Along the 2200 km pipeline are about 13 compressor stations. (<http://www.gazprom.com/projects/srto-torzhok/>). Missing data near the coasts are due to data quality issues. Note that the official names of the compressor stations are unknown to the authors, therefore they are named after the nearest settlement.

production facilities of the Urengoy gas field are located. This is west of the Urengoyskaya power plant (E). The area around the city of Surgut (A and B in Fig. 2) also shows increased NO_x emissions that might be related to anthropogenic emissions from the city and to local natural gas drilling. Prior emission knowledge in this region is represented in the HTAP 2010 NO_x emissions. The gas compressor stations are clearly not present in the HTAP emission database. Only the power plants and the central location of the natural gas drilling are present. Furthermore, compared to DESCOP the HTAP emissions of Vorkutinskaya (F) and Nizhnevartovsk (C) are strongly overestimated, while HTAP underestimates emissions from the power plants in Surgut. In addition, in HTAP a large emission source is visible at the location of Noyabrsk (halfway between Surgut (B) and Urengoy (E), which is very weak in the DESCOP emissions. Noyabrsk is a small city of about 100,000 people with some small-scale natural gas drilling in the neighborhood, but it is unlikely to contribute to the large emissions reported in HTAP.

Emissions for the power plants in the region are rather constant over time except for Vorkutinskaya (F) and Nyagan (D), who show

decreasing emissions during this single year (see Supplementary Figs. 3 and 4). Soil-biogenic emissions in the domain are calculated from the emissions derived with DESCOP in a region of about 100 by 50 km (9×9 grid cells) in the rural area north of compressor station Verkhnekazymskiy (F). The emissions of the compressor stations are corrected for these biogenic emissions that are almost zero in winter time and increase in summer time to approximately 0.96 Mg(N) month⁻¹ per grid cell or 15 kg(N) km⁻² month⁻¹. The variability in emissions from the compressor stations is rather high and more than for the power plants, which might be related to more variable operations of gas compressor stations²². Note that north of Surgut (A and B) several elevated emissions are visible in Fig. 4 that can be linked to the many smaller gas installations and urban agglomerations in this region.

We also calculated the average NO_x emissions of each power plant in the region and the first six compressor stations along the SRTO-Torzhok natural gas pipeline (Table 2). The gas-fired power plants show NO_x emissions that scale approximately with their production capacity. Exception is Vorkutinskaya, the only coal-burning power plant. Coal burners emit approximately 14 times

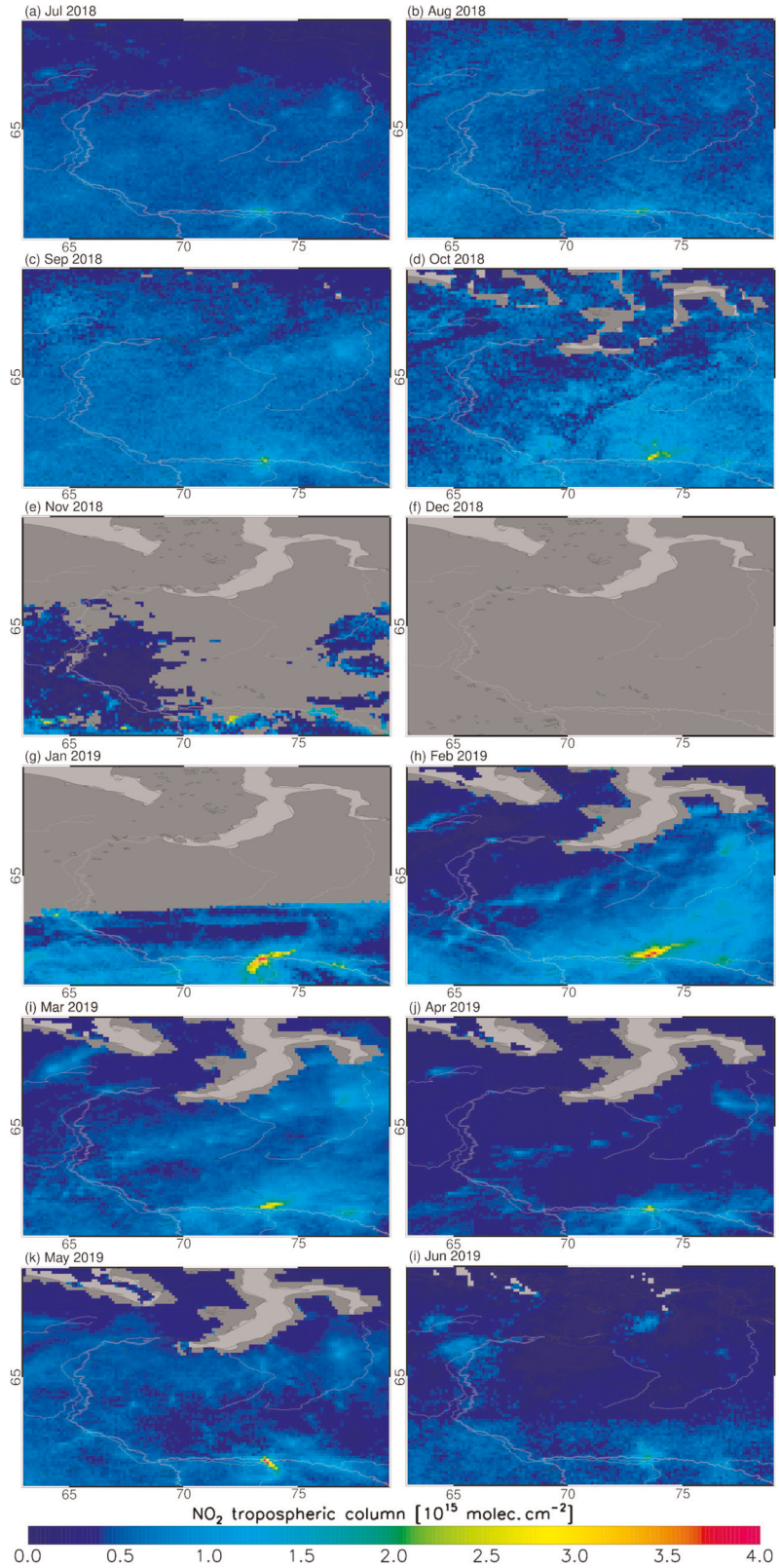


Fig. 3 Monthly mean NO₂ data over West Siberia for the months in all seasons from July 2018 to June 2019 sorted in the order of January to December. The maximum solar zenith angle allowed in the observations is 81.2°.

more NO_x than gas-fired plants²³. Emissions of Lykhma and Station 2 are about a factor two smaller than the other four compressor stations, possibly related to differences in compressor station power capacity.

The compressor stations show surprisingly large emissions of the order of 15–45 Mg(N) month⁻¹. Their NO_x emission amounts are similar to a large gas-fired power plant or a medium-size coal-burning power plant. For comparison, total emissions of a city like

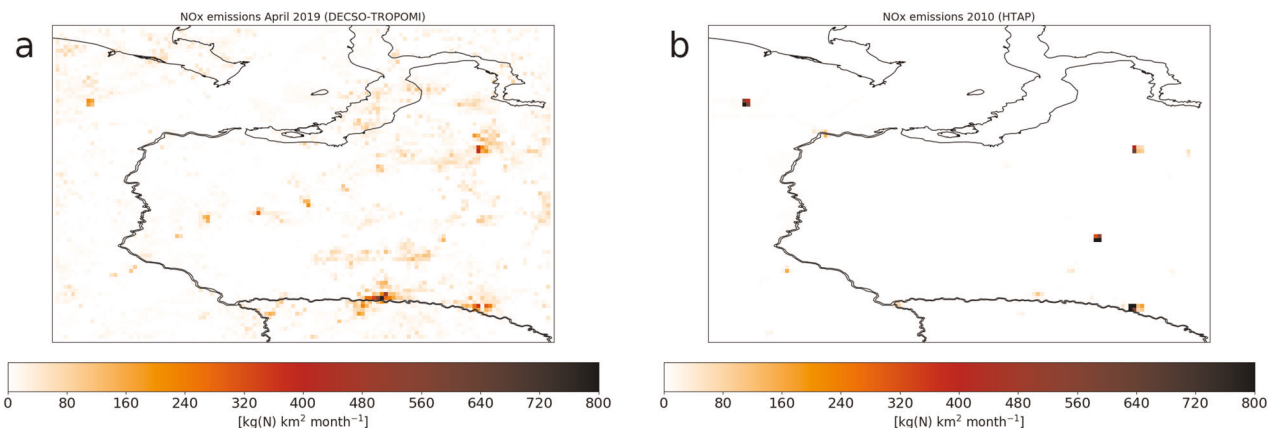


Fig. 4 NO_x emissions for April 2019. **a** Derived with the DECSO algorithm applied to TROPOMI NO₂ observations and **(b)** NO_x emissions given by the bottom-up inventory HTAP v2.2 for April 2010.

Table 2. Estimated emissions of the compressor stations and power plants in the studied region.

Compressor station	Emissions (Mg (N) month ⁻¹)
1 Pravokhettinskiy	30.0
2 Station 2	14.8
3 Priozernyy	38.9
4 Sosnovka	40.2
5 Verkhnekazymskiy	44.1
6 Lykhma	18.5
<i>Power plant</i>	
A Surgut GRES 2 (4800 MW) and CCGT (800 MW)	82.0
B Surgut GRES 1 (3280 MW)	51.1
C Nizhnevartovsk (1600 MW)	12.1
D Nyagan (1254 MW)	14.5
E Urengoyskaya (474 MW)	1.8
F Vorkutinskaya (380 MW)	16.6

Amsterdam with a population of close to 1 million have been estimated¹³ 30 Mg(N) month⁻¹.

Emission factors of compressor stations are not known in literature¹² and no other emissions estimates of the Siberian compressor stations have been reported. For the Marcellus Shale gas extraction in Pennsylvania, USA, compressor station NO_x emissions are estimated at 46–90 tons (NO_x) year⁻¹ or 1.7–3.3 Mg (N) month⁻¹ for a single station²⁴. This is an order of magnitude smaller than the emissions determined for the Siberian compressor stations. However, for shale gas extraction gas compressor stations are smaller but more numerous (200 stations). In addition, these stations are located in more populated areas—and in the USA—where more strict emission regulations are in place²⁵. Hence, the fact that emissions for single compressor stations in Siberia are larger than in the USA may not be a surprise. Information about how many compressor stations are present along the SRTO-Torzhok pipeline is hard to find. The satellite data suggest that there should be at least 25 ground stations. For the Marcellus Shale area 51.6 Mg(N) emissions per billion cubic meters of transported natural gas have been reported²⁶. The annual capacity of the SRTO-Torzhok pipeline²⁷ is 28.5×10⁹ m³. Using the emission numbers for the Marcellus shale would yield total emissions along the pipeline of 123 Mg(N) month⁻¹, suggesting emissions of ~10 Mg(N) month⁻¹ for each ground station, which is significantly

smaller than emissions per ground station derived from the satellite data (15–45 Mg(N) month⁻¹).

DISCUSSION

The new capacity for satellite observations of NO₂ over snow or ice covered surfaces has not only resulted in 23% more observations from TROPOMI, but also allows for observing NO₂ concentrations and emissions from cities, power plants, natural gas industry and soil over boreal regions like West Siberia. It also allows for the first satellite observation based estimates of soil-biogenic emissions from boreal forests (15 kg(N)km⁻² month⁻¹), which is a relevant topic of future research. The most striking finding is the large amount of NO_x emitted by gas compressor stations in West Siberia. Each gas compressor station emits in the range of 15–45 Mg(N) month⁻¹, which is more than an order of magnitude larger than for example the compressor stations of the Marcellus shale in Pennsylvania. Over the 2200 km natural gas pipeline SRTO-Torzhok, with gas compressor stations at about every 75–100 km, the total amount of NO_x emissions for natural gas transport is as much as that of a megacity or small country. Furthermore, also CO₂ is emitted proportionally to NO_x for these compressor stations. Hence, understanding emissions associated with natural gas transport are also relevant from a climate perspective.

These results highlight new possibilities and applications that the TROPOMI satellite can provide for small-scale emission monitoring. They also show that future improvement can be expected provided new satellite instrument design and better detector technology improve the signal-to-noise ratio of the measurements.

METHODS

Deriving NO₂ concentrations over snow and ice

For studying the NO₂ concentrations we are using the TROPOMI NO₂ offline data product T5-MP-DOMINO version 1.2 processed by KNMI²⁸. The algorithm calculates the total slant column with a DOAS technique. Using a data assimilation technique, the stratospheric slant column is calculated and subtracted from the total slant column. The NO₂ profile shape in the data assimilation is used to calculate a tropospheric air mass factor for deriving the tropospheric total column.

Since snow and clouds have comparable albedos in the wavelength range of our cloud retrieval algorithm no cloud fraction can be derived. Without information on the cloud fraction the correct NO₂ concentration can no longer be retrieved and that is why pixels with snow cover are filtered out of the data. This affects, especially in the winter months, a large part of the Northern hemisphere with no longer any NO₂ data available. This is rather unfortunate, as cloud free pixels with snow coverage would

lead to NO_2 retrievals of high quality because of the high reflectance of light and therefore increased signal-to-noise ratio.

In order to identify the cloud-free pixel or pixels with negligible cloud fraction over snow we use the retrieved effective cloud pressure p_{eff} . If this effective cloud pressure is close to the ground pressure p_{surf} (within the error of the retrieved pressure), we can safely assume that the pixel is cloud-free or contain only fog at ground level. We use the following criteria in which the effective cloud pressure is within 2% of the surface pressure or the cloud height is calculated as lower than the surface height:

$$p_{\text{eff}} > 0.98 p_{\text{surf}}. \quad (1)$$

Both the retrieved ground pressure and the surface pressure are part of the NO_2 data product. The retrieved effective ground pressure is derived using the O2-A absorption band in the TROPOMI spectrum and the surface pressure comes from the analyzed 3-hourly meteorological fields from the European Centre for Medium Range Weather Forecast (ECMWF) interpolated to the TROPOMI footprint²⁸. It turned out that about 60% of pixels, which were previously unused because of their snow coverage, are actually cloud-free and are with this new criteria flagged as correct NO_2 observations.

Emission estimates (DECSO)

Space-based NO_x emission estimates are derived with our in-house developed, state-of the-art algorithm DECSO (Daily Emission estimation Constrained by Satellite Observations²⁰). DECSO is specifically designed to use daily satellite observations of column concentrations for fast updates of emission estimates of short-lived atmospheric constituents on a mesoscopic scale. The algorithm needs only one forward model run from a chemical transport model to calculate the sensitivity of concentration to emissions using trajectory analysis to account for transport away from the source. DECSO is using a Kalman Filter for assimilation of the emissions, where emissions are translated to concentrations via the chemistry-transport Model CHIMERE²⁹ and compared to the observations using the averaging kernels of the NO_2 retrieval. The DECSO algorithm combines the sensitivity of NO_2 column concentrations on local and nonlocal NO_x emissions using a simplified isobaric surface 2-D trajectory analysis. The DECSO algorithm allows for calculating local and non-local sensitivities of concentration to emission based on a single forward chemistry-transport model run from the CHIMERE model, without using adjoint model code or perturbation techniques. Hence, there is no need to calculate explicitly the sensitivities or the evolution of the emission covariance. Sensitivities are available everywhere regardless whether or not there are emissions in CHIMERE. As a consequence, DECSO is able to detect new emission sources, which are not present in the a-priori emissions used by the CHIMERE model simulation. Both the 2-D trajectory analysis and the CHIMERE model use wind data from the operational data of the European Center for Medium range Weather Forecasts (ECMWF). By using a Kalman filter in the inverse step, optimal use of the a priori knowledge and the newly observed data is made. Important advantages of the DECSO algorithm are further that it can be applied to mesoscale emission inventories, and works at least for short-lived chemical species. It is fast enough to enable daily assimilation of satellite observations and provides daily emission updates. Finally, it converges sufficiently fast toward the new emission levels to enable short-term emission trend analysis. More details about the DECSO algorithm can be found in Mijling and van der A²⁰. Various versions of the DECSO algorithm have been validated in several papers^{30–32}. Based on these validation studies and calculations using the DECSO error estimates of the daily emissions, we can say that in general the uncertainty of the monthly averaged NO_x emissions is about 20%. Currently, OMI observations are used for NO_x emission estimates. For this study, we have switched to TROPOMI retrievals, taking advantage of the superior spatial resolution and signal-to-noise ratio of this instrument. Thus, a new DECSO algorithm has been developed for the processing of TROPOMI data on a higher resolution grid. To that effect, adaptations had to be made to meteorological input files, new derivations for the settings of the variances of the model and the observations and the preprocessing of the TROPOMI data. For computational reasons we have chosen for a 0.125° resolution, which corresponds to about 10 km depending on the latitude. Because of the higher spatial resolution of the grid we had to increase the temporal resolution of the trajectory analyses used for the sensitivity calculations with a factor 4. While deriving the sensitivity the effective lifetime of NO_x has been fitted in the process. The fitted lifetime was originally limited to minimum 2 h, in the version for TROPOMI we decreased the minimum lifetime to 1 h. None of the gridded fitted lifetime

variables was ever lower than 1 h. Daily emissions have been calculated for the period of 1 February 2018 to 30 June 2019. The first 5 months are rejected as spin-up time for the algorithm, resulting in 1 year of NO_x emissions (July 2018–June 2019). Since DECSO only updates the emissions based on new observations, the emissions during the polar night remain constant.

DATA AVAILABILITY

The NO_2 data of the TROPOMI instrument analyzed during the current study are publicly available in the Copernicus S5p hub at <https://s5phub.copernicus.eu/>. The HTAP data analyzed during the current study are publicly available at <https://edgar.jrc.ec.europa.eu/htap.php>. The NO_x emission data generated during and analyzed during the current study are publicly available at the GlobEmission webpage http://www.globemission.eu/region_westsiberia/datapage_nox.php.

Received: 25 September 2019; Accepted: 17 March 2020;

Published online: 14 April 2020

REFERENCES

1. Veefkind, J. P. et al. TROPOMI on the ESA Sentinel-5 Precursor: A GMES mission for global observations of the atmospheric composition for climate, air quality and ozone layer applications. *Remote Sens. Environ.* **120**, 70–83 (2012).
2. World Meteorological Organisation (WMO). *Observing Systems Capability Analysis and Review Tool* (OSCAR) (WMO, 2019).
3. Hibbitt, C. & Collison, D. Corporate environmental disclosure and reporting developments in Europe. *Soc. Environ. Account. J.* **24**, 1–11 (2004).
4. European Union, Monitoring, reporting and verification of EU ETS emissions (2019); https://ec.europa.eu/clima/policies/ets/monitoring_en (2019)
5. Directive 2008/50/EC of the European Parliament and of the Council of 21 May 2008 on ambient air quality and cleaner air for Europe (2008), <https://eur-lex.europa.eu/eli/dir/2008/50/2015-09-18> (2019).
6. Duncan, B. N. et al. A spacebased, high-resolution view of notable changes in urban NO_x pollution around the world (2005–2014). *J. Geophys. Res.* **121**, 976–996 (2016).
7. Krotkov, N. A. et al. Aura OMI observations of regional SO_2 and NO_2 pollution changes from 2005 to 2015. *Atmos. Chem. Phys.* **16**, 4605–4629 (2016).
8. Levelt, P. F. et al. The ozone monitoring instrument: overview of 14 years in space. *Atmos. Chem. Phys.* **18**, 5699–5745 (2018).
9. Li, C. et al. Recent large reduction in sulfur dioxide emissions from Chinese power plants observed by the ozone monitoring Instrument. *Geophys. Res. Lett.* **37**, L08807 (2010).
10. Lin, J.-T. & McElroy, M. B. Detection from space of a reduction in anthropogenic emissions of nitrogen oxides during the Chinese economic downturn. *Atmos. Chem. Phys.* **11**, 8171–8188 (2011).
11. Lu, Z. & Streets, D. G. Increase in NO_x emissions from Indian thermal power plants during 1996–2010: unit-based inventories and multisatellite observations. *Environ. Sci. Tech.* **46**, 7463–7470 (2012).
12. Wang, S. W. et al. Growth in NO_x emissions from power plants in China: bottom-up estimates and satellite observations. *Atmos. Chem. Phys.* **12**, 4429–4447 (2012).
13. Verstraeten, W. W. et al. Rapid increases in tropospheric ozone production and export from China. *Nat. Geosci.* **8**, 690–695 (2015).
14. Li, C. et al. India is overtaking China as the world's largest emitter of anthropogenic sulfur dioxide. *Sci. Rep.* **7**, 14304 (2017).
15. Wang, S. et al. Satellite measurements oversee China's sulfur dioxide emission reductions from coal-fired power plants. *Environ. Res. Lett.* **10**, 114015 (2015).
16. de Foy, B., Lu, Z. & Streets, D. G. Satellite NO_2 retrievals suggest China has exceeded its NO_x reduction goals from the twelfth five-year plan. *Sci. Rep.* **6**, 35912 (2016).
17. van der A, R. J. et al. Cleaning up the air: effectiveness of air quality policy for SO_2 and NO_x emissions in China. *Atm. Chem. Phys.* **17**, 1775–1789 (2017).
18. Reuter, M. et al. Towards monitoring localized CO_2 emissions from space: co-located regional CO_2 and NO_2 enhancements observed by the OCO-2 and S5P satellites. *Atmos. Chem. Phys.* **19**, 9371–9383 (2019).
19. WRI (World Resources Institute). <http://datasets.wri.org/dataset?q=power+plants> (2019).
20. Mijling, B. & van der A, R. J. Using daily satellite observations to estimate emissions of short-lived air pollutants on a mesoscopic scale. *J. Geophys. Res.: Atmos.* **117**, D17302 (2012).
21. Janssens-Maenhout, G. et al. HTAP_v2.2: a mosaic of regional and global emission grid maps for 2008 and 2010 to study hemispheric transport of air pollution. *Atmos. Chem. Phys.* **15**, 11411–11432 (2015).
22. Kurz, R., Lubomirsky, M. & Brun, K. Gas compressor station economic optimization. *Int. J. Rotating Machinery* **2012**, 9 (2012).

23. de Gouw, J. A., Parrish, D. D., Frost, G. J. & Trainer, M. Reduced emissions of CO₂, NO_x and SO₂ from U.S. power plants owing to switch from coal to natural gas with combined cycle technology. *Earth's Future* **2**, 75–82 (2014).
24. Litovitz, A., Curtright, A., Abramzon, S., Burger, N. & Samaras, C. Estimation of regional air-quality damages from Marcellus Shale natural gas extraction in Pennsylvania. *Environ. Res. Lett.* **8**, 1 (2013).
25. Environmental Protection Agency, Oil and Natural Gas Sector: Emission Standards for New, Reconstructed, and Modified Sources; Amendments (2018), https://www.epa.gov/sites/production/files/2018-03/documents/fn Og_amendments_final_rule_0.pdf (2019).
26. Roy, A. A., Adams, P. J. & Robinson, A. L. Air pollutant emissions from the development, production, and processing of Marcellus Shale natural gas. *J. Air Waste Manag. Assoc.* **64**, 19–37 (2014).
27. Gazprom, <http://www.gazprom.com/projects/urengoyskoye/> (2019).
28. van Geffen, J. H. G. M., Eskes, H. J., Boersma, K. F., Maasakkers, J. D. & Veefkind, J. P. TROPOMI ATBD of the total and tropospheric NO₂ data products, SSP-KNMI-L2-0005-RP, issue 1.4.0 (2019).
29. Menut, L. et al. CHIMERE 2013: a model for regional atmospheric composition modelling. *Geoscientific Model Dev.* **6**, 981–1028 (2013).
30. Ding, J. et al. Intercomparison of NO_x emission inventories over East Asia, *Atm. Chem. Phys.* **17**, 10125–10141 (2017).
31. Ding, J., van der A, R. J., Mijling, B. & Levelt, P. F. Space-based NO_x emission estimates over remote regions improved in DECSO, *Atmospheric. Meas. Tech.* **10**, 925–938 (2017).
32. Ding, J. et al. Maritime NO_x emissions over Chinese seas derived from satellite observations. *Geophys. Res. Lett.* **45**. <https://doi.org/10.1002/2017GL076788> (2018)

AUTHOR CONTRIBUTIONS

R.v.d.A conducted the data analysis, developed the DECSO inversion algorithm for TROPOMI, and was lead author of the paper, A.d.L conducted the data analysis and co-authored the paper, J.D was responsible for developing the DECSO inversion algorithm for TROPOMI, H.E. was responsible for the TROPOMI NO₂ retrievals.

COMPETING INTERESTS

The authors declare no competing interests.

ADDITIONAL INFORMATION

Supplementary information is available for this paper at <https://doi.org/10.1038/s41612-020-0119-z>.

Correspondence and requests for materials should be addressed to R.J.v.d.A.

Reprints and permission information is available at <http://www.nature.com/reprints>

Publisher's note Springer Nature remains neutral with regard to jurisdictional claims in published maps and institutional affiliations.



Open Access This article is licensed under a Creative Commons Attribution 4.0 International License, which permits use, sharing, adaptation, distribution and reproduction in any medium or format, as long as you give appropriate credit to the original author(s) and the source, provide a link to the Creative Commons license, and indicate if changes were made. The images or other third party material in this article are included in the article's Creative Commons license, unless indicated otherwise in a credit line to the material. If material is not included in the article's Creative Commons license and your intended use is not permitted by statutory regulation or exceeds the permitted use, you will need to obtain permission directly from the copyright holder. To view a copy of this license, visit <http://creativecommons.org/licenses/by/4.0/>.

© The Author(s) 2020